Lab on a Chip

PAPER

View Article Online
View Journal | View Issue

Cite this: *Lab Chip*, 2025, **25**, 2744

An integrative round window membrane/cochlear microphysiological system with sensing components for the study of real-time drug response†

Jing Bai, * Olurotimi Bolonduro, Pavlo Gordiichuk, R. Madison Green, Henry Hung-Li Chung, Ken Mahmud and Dmitry Shvartsman

Most hearing loss often results from permanent damage to cochlear hair cells, and effective treatments remain limited. A reliable, scalable, and physiologically relevant ear model can accelerate the development of hearing-loss protection therapeutics for injury prevention and hearing restoration. The challenge remains on screening delivery systems for regenerative compounds, and no *in vitro* screening systems exist that capture the complexity of inner ear properties. Here, we present a high-throughput, microphysiological system (MPS) featuring a round window membrane (RWM) model co-cultured with murine auditory hair cells. It is integrated with a transepithelial electrical resistance (TEER) sensor module to monitor epithelial barrier function development in continuous measurements, without sacrificing a sample and thus allowing "real-time" monitoring of the RWM construct progress. The MPS integrates a syringe pump, tissue compartment, multi-channel fluid distributor, and sensors into a microfluidic continuous-flow system, allowing for on-demand sample collections of analytes triggered by the cellular response to the introduced compounds. Drug screening was conducted with protective antibiotic, antioxidant, and anti-inflammatory compounds. RWM cell and hair cell viability, TD_{50} values, and membrane integrity were measured. In addition, we also designed a graphene field-effect transistor (GFET)-based cytokine sensor to study proinflammatory cytokine release from cells during damaging exposure. The system was employed to assess drug diffusion efficiency, cell viability, and the drug's TD_{50} and compared to published data from animal studies. Cell membrane integrity was also analyzed, and proinflammatory cytokine release was measured using a GFET sensor. We evaluated and monitored the real-time structural integrity of the RWM epithelial barrier using the integrated TEER sensor in the MPS. The sensor's ability to measure TEER and cytokine levels was validated by comparing its readings to those obtained from commercial TEER signal processing equipment and standard cytokine concentration measurements. This ear-on-a-chip design enables high-throughput screening of investigational new drugs, reducing the need for animal models in complex studies of inner ear damage and regeneration. It allows for the real-time study of drug responses. It facilitates the development and identifying novel agents that protect against hearing loss and the design of delivery methods for hearing regeneration compounds.

Received 2nd December 2024,
Accepted 25th April 2025

DOI: 10.1039/d4lc01025f

rsc.li/loc

Introduction

Today, over 5% of the world's population has disabling hearing loss, 432 million adults and 34 million children and it is estimated that by 2050 over 900 million people – or one in every ten people – will have irreversible hearing loss. Despite these numbers, no Food and Drug Administration (FDA)-approved drug is available for the treatment or prevention of noise-induced hearing loss (NIHL).[1]

The inner ear is protected by barriers like the blood-labyrinth barrier (BLB), which makes it difficult for systemically administered drugs to reach therapeutic levels in the cochlea or vestibular system. One of the current drug delivery routes for the inner ear (oto drug delivery) is delivered near the round window membrane (RWM), which acts as a gateway for diffusion into the cochlea (Fig. 1A). The RWM is a tri-layer structure made of an outer mucosal epithelium, a middle core of connective tissue, and an inner squamous epithelium.[2] Drugs applied near the RWM can diffuse through the membrane,

Department of Living Systems, Triton Systems, Inc., Chelmsford, MA, USA. E-mail: jbai@tritonsys.com

† Electronic supplementary information (ESI) available. See DOI: https://doi.org/10.1039/d4lc01025f

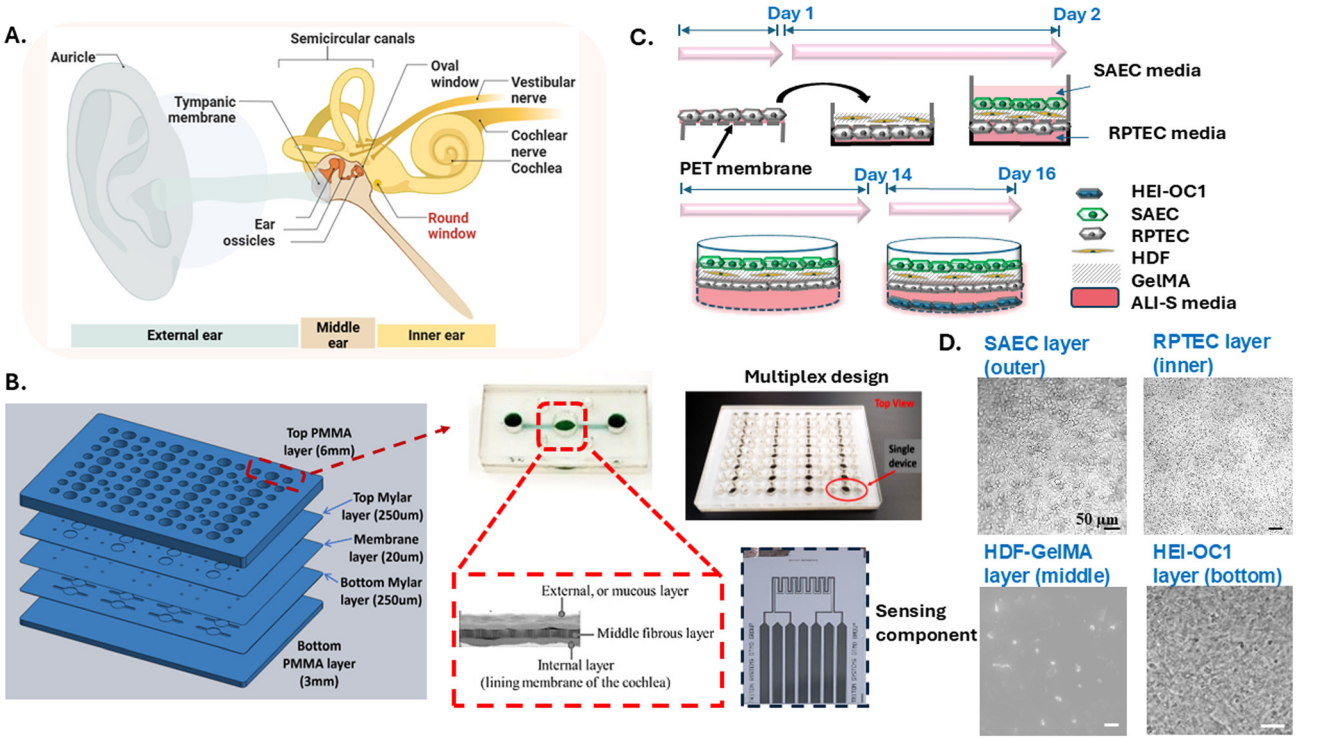

Fig. 1 Design layout and the characterization of the integrated RWM/cochlear platform. A. Images of inner ear structure. B. Schematic sketch of the integrated platform (with single/multiplex design and sensor components). C. Illustration of cell seeding procedure. D. Images of the RWM cell layers and HEI-OC1 hair cells.

allowing therapeutic agents to reach the inner ear fluids (perilymph) and target the cochlear structures. This route is advantageous because it bypasses systemic circulation, reducing potential systemic side effects while enabling localized, high-concentration drug delivery. Auditory hair cells are specialized sensory cells located in the cochlea of the inner ear, responsible for converting sound vibrations into electrical signals that are transmitted to the brain. Damage to these cells, often due to aging, noise exposure, or ototoxic drugs, leads to hearing loss, as hair cells do not regenerate in humans. Hence, there is a critical need for the development of effective therapeutics against hearing loss,[3] and prevent auditory hair cell damage.

While the use of otoprotective drugs is intuitive, there are numerous challenges in the translation of promising therapeutic candidates into human clinical testing. Those challenges include delivery, physicochemical properties to cross barriers, and lack of reliable molecular targets.[4] Underlining these discouraging drug discovery and commercialization trends are the lack of organotypic *in vitro* models that would enable high throughput screening of viable therapeutics candidates, and the ambiguity of the translational relevance of available animal models.[5] The FDA's 3R (replace, reduce, refine) initiative highlights the importance of minimizing animal testing by promoting alternative methods that reduce animal use while improving the reliability of preclinical data.

Microfluidic-based 3D cell culture assays (microphysiological systems – MPS) have been extensively developed to address different biomedical problems, offering advantages in terms of real-time imaging, miniaturization and controllable biophysical and biochemical microenvironments. MPS can significantly reduce the cost and risk associated with animal testing by identifying ineffective or toxic compounds early in the drug development pipeline. Historically and in a majority of current studies, preclinical middle-inner ear research relies on rodent models (chinchilla and murine). Recently, larger animals like pigs and sheep have gained attention due to their auditory similarities to humans.[6] Due to the cost, ethical concerns and scale-up limitations of current preclinical models, there is a growing interest in developing 3D *in vitro* models of the RWM and cochlear. One of them has been developed using a 3-layer of Madin Darby canine kidney (MDCK) cells co-cultured with fibroblasts to mimic the structure of the RWM in a conventional Transwell model.[7] Very recently, a cochlear organoids-integrated conductive hydrogel biohybrid system with cochlear implant electroacoustic stimulation (EAS) for cochlea-on-a-chip construction and high-throughput drug screening has been developed.[8] Another study has designed a BLB from post-mortem human tissue and established an endothelial cell and pericyte culture system on a BLB chip.[9] However, current systems lack a comprehensive approach for integrating RWM with the cochlear, which is essential for mimicking the complex interactions between the middle and the inner ear. Additionally, these models lack the capability for non-invasive, real-time detection of the epithelial barrier functions and biomarkers associated with cellular responses to drugs.

One of the most important aspects of MPS is the on-chip sensor suits.[10] It provides real-time, quantitative, and non-

invasive monitoring of biological processes. Transepithelial electrical resistance (TEER) measurement is a convenient and reliable way to monitor the development of tight junction, integrity, and formation of intact epithelial monolayers in a time-dependent manner. This method can also provide information about the permeability of biomolecules or drugs upon changes in the integrity of the tight junctions. In addition, graphene-based field effect transistor (GFET) protein sensors offer significant advantages due to their low cost, flexibility in detection strategy development, and broad applicability, are also being proposed for use in microfluidic devices for MPS studies.[11,12] Detecting epithelial barrier function and inflammatory cytokines in real-time with integrated sensors is crucial for understanding the dynamic cellular responses in the presence of drugs, which can provide valuable insights into drug usage.

In this study, we developed a novel first-generation *in vitro* 3D middle ear/cochlear-on-a-chip microphysiological system (MPS) model to address the current limitations of existing models, using animal models and lack of *in vitro* alternatives that enable a high-throughput screening. We successfully incorporated a three-layered RWM and auditory hair cell model within a microfluidic setup, achieving maturation of the tissue phenotype. The initial choice of cells for the RWM model was driven by basic requirements of tissue stability over a prolonged period (up to 21 days) in standard tissue culture conditions, establishment of a non-permeable cell barrier that mimics round window diffusion properties, ease of use and a need to have a variety of initial cell response assays for assessing selected drugs activity. We understand that the current model has its limitations for replicating a complete biological architecture of the RWM and will benefit from inclusion of vascular and immune components, which we hope to achieve in the next generation models.

Additionally, we designed and validated multiplex device performance with 16 and 32 units that fit conventional tissue culture plates, integrating multi-well TEER sensors and GFET protein sensors.

We designed a multiplex fluid distributor to control the MPS's media distribution. For drug testing, we conducted initial toxicity screenings of four common therapeutics for treating middle ear infections and reducing inflammation—erythromycin, gentamicin, dexamethasone, and ciprofloxacin—using the RWM-on-a-chip model. They were selected because of therapeutic relevance and varied in chemical structure, diffusion properties, and molecular weights. Toxicity was evaluated through Live/Dead assays and lactate dehydrogenase (LDH) assays. We calculated the TD_{50} values for ciprofloxacin in the RWM model and compared our data to published work to validate our system. Those assays developed in the MPS demonstrated that our round window membrane MPS is a reliable and robust platform for assessing drug toxicity.

The integration of HEI-OC1 hair cells[13] allows for testing the hair cell drug responses to common anti-inflammatory medications like dexamethasone, as well as novel antioxidant compounds such as hyaluronan-antioxidant conjugates – glutathione–HA and cysteine–HA.[14] We performed dose–response hair cell viability tests using the Celltiter-Glo assay. Additionally, we successfully assessed the diffusion of common antibiotics and anti-inflammatory drugs across the RWM layer using LC-MS/MS, demonstrating the permeability of our model and comparing the results with *in vivo* data.[15,16] Using TNF-α as a reference, we validated accurate measurements of protein concentrations in cell culture media. This approach enables high-throughput screening of investigational new drugs while reducing reliance on animal models, facilitating the development and identification of novel protective agents against hearing loss.

Results and discussion

Optimization of the RWM/cochlear MPS and fluidic distributor design

The round window membrane separates the middle and inner ear parts (Fig. 1A). And we designed the RWM/cochlear MPS in both single and multiplex design versions. The multiplex device was designed for high-throughput drug analysis – there are 32 identical functional units (16 units for TEER units). Each functional unit is identical to the singular format, with a membrane separating the top chamber and the bottom channel.

We've designed a two-channel microfluidic device prototype, shown in Fig. 1B. It consists of an open-top top chamber and a closed basal channel with two openings for cell culture media perfusion. A porous polyester (PET) membrane separates the upper well and bottom channel, creating distinct chambers for cell growth. We created the RWM tissue analogs on a chip-triculture of primary human small airway epithelial cells (SAEC), primary human dermal fibroblasts (HDF) encapsulated in 7.5% GelMA, and primary human renal proximal tubule epithelial cells (RPTEC). We seeded abundant SAEC to form a multilayer structure, replicating the physiological architecture and function of the *in vivo* RWM. After SAEC and RPTEC formed intact layers, we introduced air–liquid interface (ALI) culture in the tissue constructs by removing cell culture media from the top chamber of each unit, and ALI media was used. The ALI culture was maintained for 14 days (Fig. 1C) before the introduction of hair cells. The phase-contrast images of all cell types are shown in Fig. 1D. Both the SAEC and RPTEC form intact layers in co-culture conditions, as well as HEI-OC1 cells, while HDF were growing in the middle gel layer (Fig. 1D).

We optimized the bottom channel geometry and the layout. The initial rectangular design of the bottom channel encountered challenges due to significant air bubble formation, which compromised system performance. To address this issue, we implemented a novel design modification by altering the channel geometry to a diamond shape. This structural change has proven highly effective in expediting the removal of air bubbles generated within the channel, resulting in a substantial improvement in system reliability and efficiency (Fig. S1†). We also found out that plasma treatment and coating with collagen

I prior to RPTEC seeding significantly improved the cell survival and formation of a monolayer on the PET membrane (Fig. S2†).

To facilitate media perfusion/drug injection on the multiplexed plate, and to decrease the number of tubing attached to the multiplexed plate, we designed a novel fluid distribution cover that can feed the media to each device with a minimum number of connected tubing (Fig. 2A and B). This fluid distribution plate was attached to the top surface of the multiplexed plate. Fig. S3A† shows a section of the fluid distribution layer to connect the bottom channel inlets of all 32 devices. There is only 1 port used for tubing connection instead of 32 individual ports for each device. As shown in Fig. S3A,† the channel lengths reaching each device are designed equally to ensure the same hydraulic resistance for each device and the same volume of liquid was distributed in each tissue unit. Fig. S3B† below shows the experimental snapshots that we validated filling off all 32 devices with a color dye (green), with the connection to our automated pump system. With $n = 4$ experiments, we validated that all 32 devices received the liquid successfully, no empty devices were left, and no leakage was observed. We believe this design is important because it significantly reduces the number of tubing lines needed to supply all devices in the multiplexed plate. And the devices are filling sequentially in less than 5 minutes.

We also showed that the shear stress mimics physiological conditions with a simulation model. Due to sound wave frequency and cochlear mechanics, the pressure drop per unit length in the cochlear fluid flow is pulsatory and proposed to be in the range of 8.9×10^{0}–1.3×10^{4} Pa m^{-1}.[17] The cochlea can sustain up to 1.5 Pa shear stress without damage[17] and the viscosity of perilymph is similar to that of water.[18] COMSOL Multiphysics modeling demonstrated that an applied flow rate of 0.1 ml min^{-1} (an optimal speed that is high enough to ensure effective sensor detection while remaining low enough to prevent cellular damage) resulted in a homogeneous distribution in the microfluidic devices, with a flow speed of 0.001–0.003 m s^{-1} within the hair cell channel (Fig. 2C and D). Next, we performed a flow-structure analysis to evaluate the impact of flow velocity on cell shear stress. The results indicate that the shear stress value remained below 0.2–0.3 Pa, which falls within the physiological safe range. This shear stress level is insufficient to cause structural deformation of the cells or tissues (Fig. S4†) in this case.

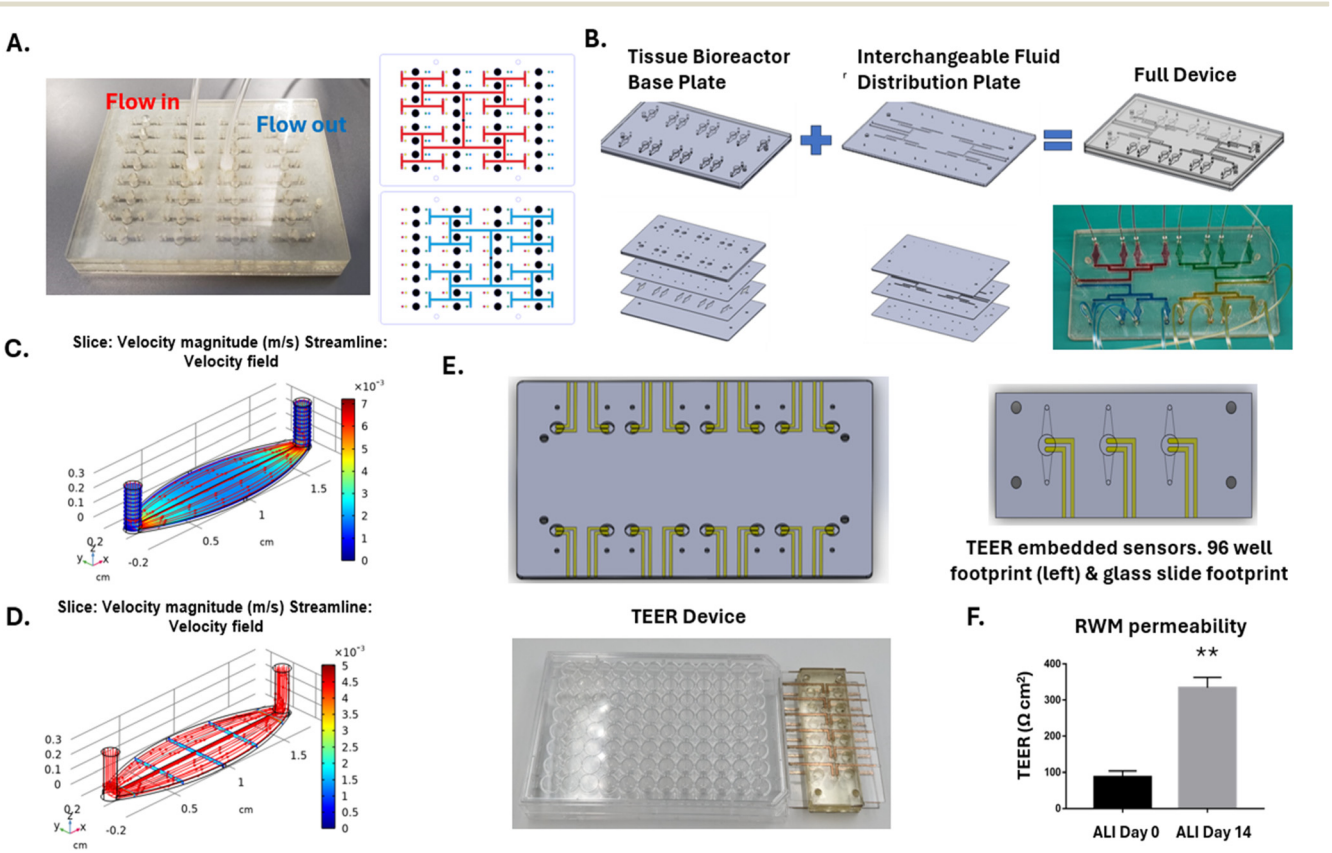

Fig. 2 Multiplex fluid distributor and TEER sensor design and validation. A. The image of the fluid distribution layer and the design (for a 32-unit device). Fabricated multiplexed plate with fluid distribution layer connecting the inlets and outlets of the bottom channels. Red-bottom inlet, blue-bottom outlet. B. Fabrication of the MPS with interchangeable fluid distribution plate (for a 16-unit device) and validation of the fluid distribution using 4 different colors, allowing for 4 different experiments with 4 replicates simultaneously. (C) The 3D COMSOL model demonstrated the *xy*-cross section of the microfluidic device, indicating homogeneous flow. (D) Similarly, the *yz*-cross section showed that the flow is stronger in the middle of the channel, reaching a speed of 0.005 m s^{-1}, while the flow at the surface is slower, with a speed of 0.001 m s^{-1}. E. TEER sensor design and image. F. RWM permeability measured using the integrated TEER from day 0 to day 14 in the air–liquid interface (ALI) culture.

TEER and protein sensors for minimally invasive RWM monitoring

We have developed a multiplex plate consisting of an 8 × 2 array of microfluidic culture zones. A close-up view of an individual culture region is shown in Fig. 2E. In this design, the TEER sensors are fabricated directly on the apical and basal surfaces of the microfluidic flow region. The pattern for this device fits within the dimensions of a 96-well plate but allows flexibility to run parallel experiments (Fig. 2E). We used this TEER device to measure the RWM barrier integrity on day 0 and day 14 in the ALI-culture. The observed increase in TEER from day 0 to day 14 in the air–liquid interface (ALI) culture indicates progressive barrier formation and cellular maturation. The TEER value in our model closely matches the *in vitro*/*ex vivo* measurements observed in the RWM[19] at day 14 (*in vitro*: 331 Ω cm^2, *ex vivo*: 305 Ω cm^2), indicating that our model effectively replicates the physiological barrier properties of the RWM.

As the position of the electrodes is fixed in the device, we eliminate variation due to positioning or working distance between electrodes. In addition to the fact that the system can be used within closed microfluidic channels & open well cultures, this system has advantages over the WPI chopstick electrodes system – especially when multiplexed testing is factored in. These measurements were performed on a MultiEmstat4 potentiostat (BioLogic, France, high range 200 kHz EIS, 4 channels) with the parameters shown in Fig. S5.† Prior to data collection, a calibration test was conducted on the instrument to ensure sensitivity, accuracy, and stability. This was carried out with a potentiostat dummy cell (a pre-built circuit with known resistors and capacitors) to validate that the instrument is working properly.

When sweeping over a large frequency range (1 Hz–1 MHz), the impedance value is dominated by different components of the equivalent circuit. At low frequencies (<100 Hz), the impedance is dominated by electrode capacitance. At higher frequencies (>100 kHz+), the impedance is dominated by the resistance of the cell culture media. The resistive plateau observed within the middle region is attributed to the presence of tight junctions within the monolayer. The values of C_E and R_{medium} will remain consistent, regardless of the integrity or maturity of the cell monolayer. Once obtained, R_{TEER} can be normalized by the cross-sectional area of the culture space. Representative EIS spectra are depicted in Fig. S6,† in which the R_{TEER} value of 15.2 Ω cm^2 was calculated from the SAEC monolayer on day 8. The embedded TEER sensor data was validated against the WPI chopstick electrodes system in a Transwell setup, and a similar value was obtained (data not shown). This testing experiment was performed without ALI culture with a lower cell seeding ratio (10 000 cells per device), higher R_{TEER} values were obtained from a fully mature tissue culture with a multi-layer (Fig. 2F). It is important to highlight that, due to instrument limitations, stimulation currents in the nA range were implemented, as opposed to the more commonly used μA range. This is a contributor to measured impedance and is important to account for when comparing TEER values from different measurement modalities.

Meanwhile, we also developed a protein GFET sensor, and we used the proinflammatory cytokine TNF-α as an example to demonstrate the proof of the feasibility of the integrated MPS platform (Fig. S7†).

Intact layers of RPTEC and SAEC formed in the RWM model

After the development of the sensors, we next characterized the MPS model at the cellular level. We first assessed RWM cell viability using the Live & Dead assay in co-culture. We found that from day 3 to day 14, there was no significant reduction in cellular viability for all cell types (Fig. S8† and 3A). We also evaluated cell cultures in the high-throughput devices. Live & Dead assay shows that there was not much cell death for a longer period of culture (Fig. S9†), with similar results we observed in the singular devices. We concluded that the successful cell seeding rate was over 90% for all 32 units, in terms of cell viability and epithelial cell monolayer formation. This indicates that we have developed a robust high-throughput RWM model for possible drug screening.

The outer mucosal epithelial cell layer plays a critical role in the round window membrane, acting as the primary barrier that regulates diffusion rates and maintains selective permeability.[20] This cell layer is key to controlling the passage of molecules through the membrane, as its tight junctions provide a robust structural integrity that restricts unwanted diffusion and enables precise cellular signaling. By forming a tight barrier, mucosal epithelial cells ensure the stability of the membrane environment, supporting effective communication between compartments while protecting sensitive inner ear tissues from external substances. Their unique properties make them indispensable for maintaining the physiological balance essential for proper auditory function. In our model, SAEC serves as the mucosal cell type (the outer layer) with a multi-layer configuration as it closely replicates the histological features of the native tissue layer.[21] For the inner squamous epithelial layer, we used RPTEC because renal epithelial cells have been used for this purpose[7] as a structural representative. The GelMA matrix with fibroblast cells serves as the connective tissue layer between the outer and inner epithelial cell layers.

Cell characterization included immunofluorescent staining the cells for the presence of the following proteins: vimentin, fibroblast marker; cytokeratin-5 (CK5) and cytokeratin-14 (CK14), epithelial markers; ZO-1, tight junction marker, MUC5AC, mucus cell marker, and beta-tubulin IV, cilia cell marker (Fig. 3B). We characterized SAEC differentiation in co-cultures under ALI conditions for the RWM model. SAEC exhibited tight junction barrier formation, epithelial cell marker expression, ciliated cell, and mucus-producing goblet cell formation on day 14 of ALI culture. Meanwhile, HDF cells exhibited their spindle-shaped morphology and expressed vimentin. RPTEC in co-culture

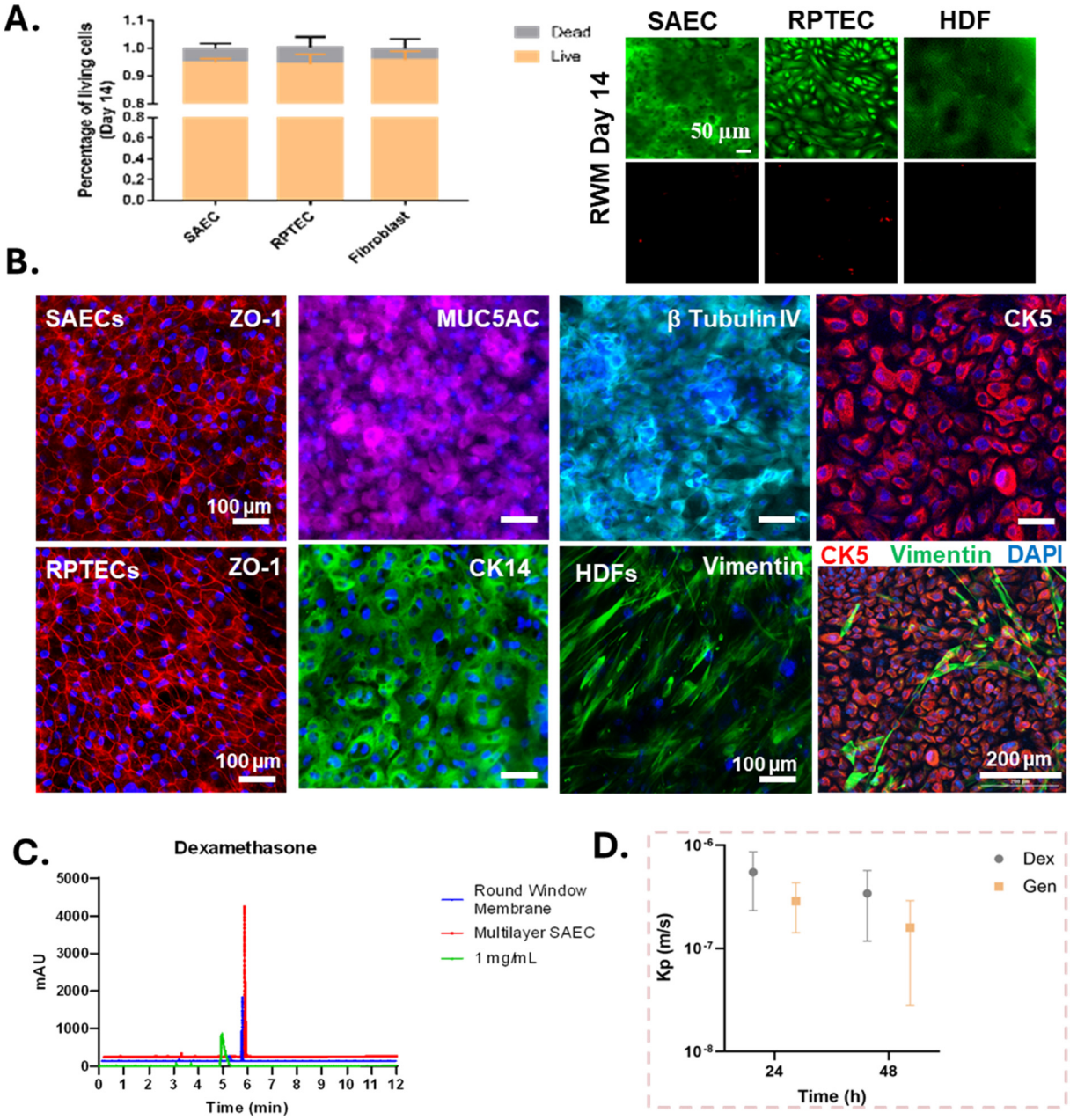

Fig. 3 Characterization of the RWM cell model and RWM drug delivery. A. Live & Dead assay – cell viability (left: quantitative analysis of individual RWM cell types in co-culture; right: images of cell viability. Green – live cells, red – dead cells). B. IF staining (each cell layer) – key marker expression 14 days post-ALI culture. SAEC was characterized by ZO-1, MUC5AC, beta-tubulin IV, and CK5; RPTEC was characterized by ZO-1 and CK14; HDF was characterized by vimentin. The lower-right image displays a projection of HDF cells cultured beneath the SAEC layer. C. Drug diffusion across the RWM barrier (LC-MS/MS) indicated a shift of peaks in the chromatogram in the presence of RWM cell type (blue: 3 cell layer, red: SAEC mucosal cell layer only, green: drug standard without cell). D. Drug permeability analysis across the RWM barrier (LC-MS/MS). Dex – dexamethasone, Gen – gentamicin.

were characterized by the formation of cell-to-cell adhesions and squamous cell types (CK14). The results showed that the intact layers with RPTEC and SAEC were maintained when 7.5% GelMA was used to construct the three-layered structure of the RWM. We also tested different concentrations of GelMA and found that 7.5% GelMA concentration facilitated speedy epithelial barrier formation and long-term culture (data not shown).

Drug diffusion validated the presence of an *in vivo*-relevant RWM model

From the LC-MS analysis, all drug retention times (RT) were between 5 and 6 minutes. Interestingly, dexamethasone RT shifted by 1 minute compared to standard (1 mg mL^{-1}). The drug formulation used was dexamethasone phosphate and the phosphate was removed following interactions with RWM

cell types (Fig. 3C). This caused the observed shift in RT and a change in mass when identified on the mass spectrometer. The other drug tested (gentamicin) retained its retention times with varying degrees of concentration after diffusion (data not shown). This can be attributed to each compound's unique chemical properties interacting with cells in the models. The data indicated that having an RWM layer in cochlear drug testing is essential, as it provides a realistic model of how drugs will interact within the ear cell types. The RWM acts as a barrier and gateway for substances entering the cochlea, influencing drug diffusion, metabolism, and potential ototoxic effects. We also evaluated the permeability and absorption of dexamethasone and gentamycin across the round window membrane model. Results showed that the drug permeability for dexamethasone and gentamicin was 5.47×10^{-7} m s^{-1} and 2.88×10^{-7} m s^{-1} at 24 h, respectively, and 3.42×10^{-7} m s^{-1}, 1.6×10^{-7} m s^{-1} for 48 h groups (Fig. 3D). Both drugs continued to accumulate in the bottom chamber until they reached equilibrium even up to 48 h. Dexamethasone exhibited a higher permeability compared to gentamycin, and these results are aligned with the published *in vivo*/*ex vivo* data.[15,16] This notable difference in permeability can be attributed to the distinct chemical properties and

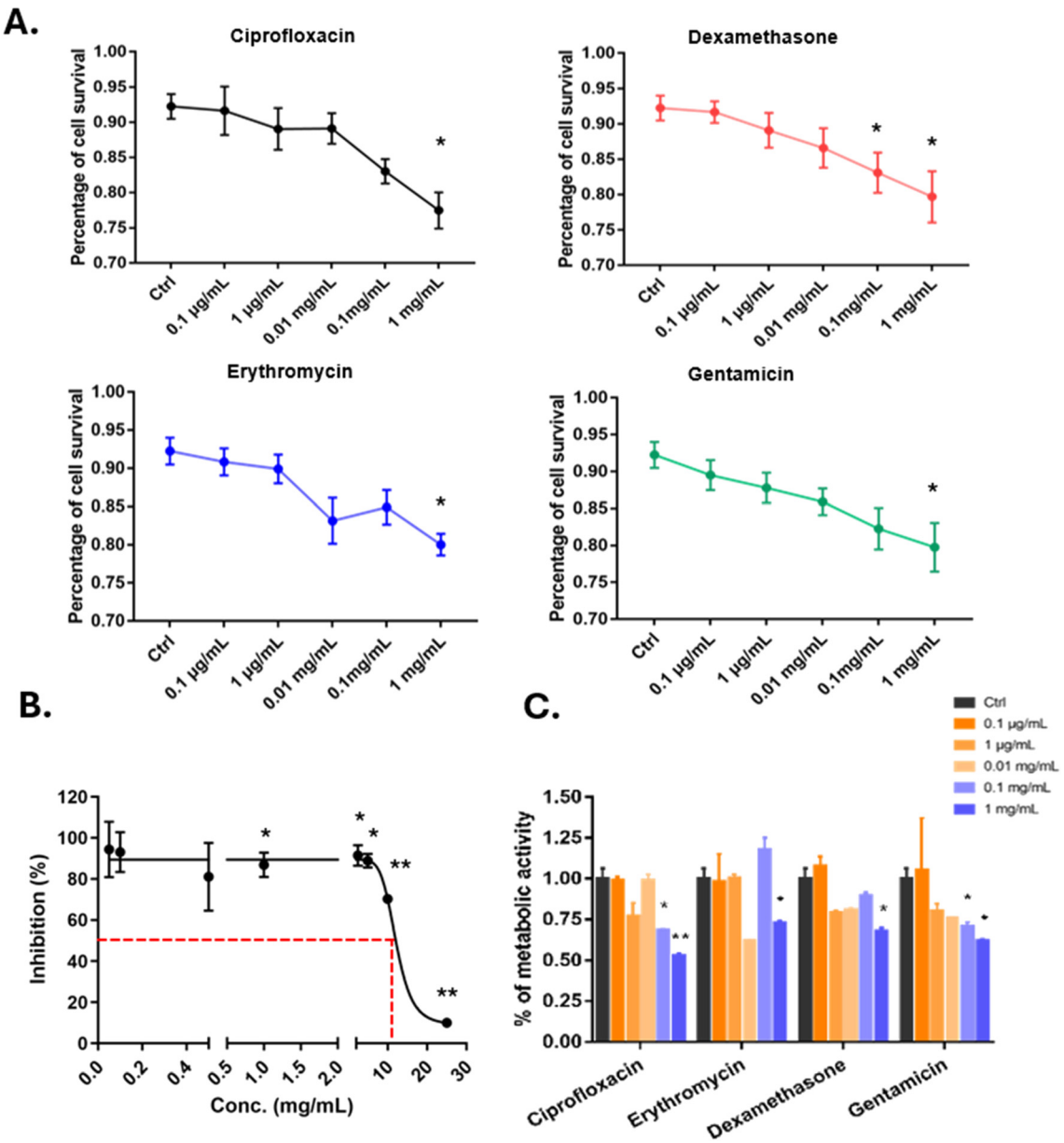

Fig. 4 Cellular drug response in the RWM model. A. Live/Dead assay – cell viability in the presence of drugs in various doses; B. TD_{50} analysis of drug-ciprofloxacin; C. LDH assay – membrane integrity in the presence of drugs. Statistical significance was determined using Student's *t*-test for pairwise comparisons between each treated group and its control group. *p*-Values <0.05 were considered statistically significant. Significance is indicated as $*p < 0.05$, $**p < 0.01$.

interactions of the two drugs with the cellular components of the membrane. Our data suggested that the designed RWM structure would adequately represent the RWM in terms of drug permeation and tissue structure.

Drug cytotoxicity testing in the RWM model

For drug dose–response analysis, we tested 4 drugs: erythromycin, gentamycin, dexamethasone, and ciprofloxacin with 5 doses each (1 mg mL^{-1}, 0.1 mg mL^{-1}, 0.01 mg mL^{-1}, 1 μg mL^{-1}, 0.1 μg mL^{-1}) up to 48 hours and the cell viability was shown in Fig. 4A. From the experiments, we noticed that cell viability was decreased as the drug concentrations increased for all 4 drugs. However, at this concentration range, none of the drugs show a significant decrease in cell survival (>50%).

Ciprofloxacin was selected as an example to demonstrate the feasibility of our RWM MPS for testing the drug TD_{50}. We found that the concentration of 25 mg mL^{-1} is sufficient to kill most of the cells at 48 hours. The percentage of cell growth inhibition in the presence of drugs was compared to the control group (without drug treatment, 100%) (Fig. 4B). From our experiment, the TD_{50} for ciprofloxacin in the tri-culture RWM model is 10.75 mg mL^{-1} (32.4 mM), indicating that it is generally well-tolerated. Specific *in vivo* LD_{50} data for intratympanic administration of ciprofloxacin are lacking, but *via* other routes, it is believed that the value is ~5000 mg kg^{-1}.[22] It was reported that ciprofloxacin has an *in vitro* TD_{50} (in terms of LC_{50}, lethal concentration that kills 50% of the cell population) of ~6 mg mL^{-1} in C6 cell line – a rat glioblastoma cell line.[23] And it shows that the data generated from our tissue construct aligns with the previous findings. However, we do need to notice that the co-culture systems may alter drug sensitivity, requiring higher concentrations for effects, selective cytotoxicity for different cell lines, and barrier prevention of drug diffusion to the basal side.

To fully analyze the behavior of our membrane tissues, we evaluated the potential damaging effects (membrane integrity) of the drugs on the cells using a Lactate Dehydrogenase (LDH) assay. We noticed that membrane integrity was decreased as the drug concentrations increased for all 4 drugs (Fig. 4C). Usually, the membrane integrity of cells is interpreted as a cell viability measurement. The membrane integrity results resemble the results from the cell viability assay using the Live & Dead assay, indicating that our model is robust and repeatable for drug toxicity tests.

Auditory hair cell integration indicated cellular compatibility in the RWM model

House Ear Institute-Organ of Corti 1 (HEI-OC1) cells are derived from the auditory organ of a transgenic mouse,[13] which is one of the few mouse auditory cell lines available for research purposes. Originally proposed as an *in vitro* system for screening ototoxic drugs, these cells have been used extensively to investigate drug effects, especially cell death, survival, and proliferation. We've optimized the cell seeding conditions and co-culture conditions. The experimental study investigates the influence of varying cell seeding densities over 48 hours at a temperature of 33 °C/10% CO_2. Cells were tested with different concentrations (10 000, and 20 000 cells per device) to assess their impact on cell proliferation.

The results indicate that the 10 000 cells per device group reached the desired cell confluence within 48 hours (Fig. S10†). The co-culture was maintained at 33 °C/10% CO_2 until the HEI-OC1 cells reached 90% confluency. Then the co-culture was moved back to 37 °C/5% CO_2 before drug testing and any other downstream assays. We also tested co-culture using different cell culture media, two media conditions were evaluated: (1) standard ALI-S media and (2) a co-culture media comprising a 1 : 1 mixture of ALI-S and DMEM supplemented with 10% fetal bovine serum (FBS). The Live & Dead assay experiment results are shown in Fig. 5A and S10.† No significant differences were observed in the normalized cell viability of RWM cell types and hair cells when comparing ALI media to ALI + DMEM media supplemented with 10% FBS. However, a slight morphological change was observed in (2) – SAEC started to detach from the gel surface, and the integrity of the multi-layer appears to be impacted. The addition of FBS to the culture media may promote differentiation of airway epithelial cells, potentially leading to alterations in cell morphology and function, and ultimately affecting the integrity of the cell layer. In addition, the presence of FBS accelerated the growth of HEI-OC1 cells in coculture, which also led to the detachment of those cells from the basal channel. Therefore, we will use the ALI-S media in the co-culture for further experiments.

The immunofluorescent staining experiment showed the tight junction marker ZO-1 expression of SAEC multi-layer (mucosal cell layer) and the auditory hair cell marker prestin of HEI-OC1 cells (Fig. 5B). The structural integrity of the SAEC layers, specifically regarding tight junctions, appears to remain relatively stable, showing minimal alterations or changes in co-culture conditions, and HEI-OC1 cell exhibits a high level of prestin, suggesting that the cellular identity and characteristics of auditory hair cells in co-culture are preserved.

In addition, we also compared the middle ear epithelial cells (MEEC) and RPTEC cells in terms of biomarker expression, drug response, and TEER measurements. These cells were chosen to replace the RPTEC to develop a micro-scale inner ear system for biocompatibility and drug testing. The switch to MEEC was motivated by their origin as primary cells isolated from the human middle ear, which play a crucial role in maintaining middle ear homeostasis. And this cell type didn't express much mucosal cell marker (data not shown), however, high expression of squamous cell marker-CK14 was observed in MEEC (Fig. S11A†). Functional assays revealed no significant differences between MEEC and RPTEC in TEER values or key biomarker expression (Fig. S11 and S12†), confirming that RPTEC can replicate the essential functional characteristics of MEEC.

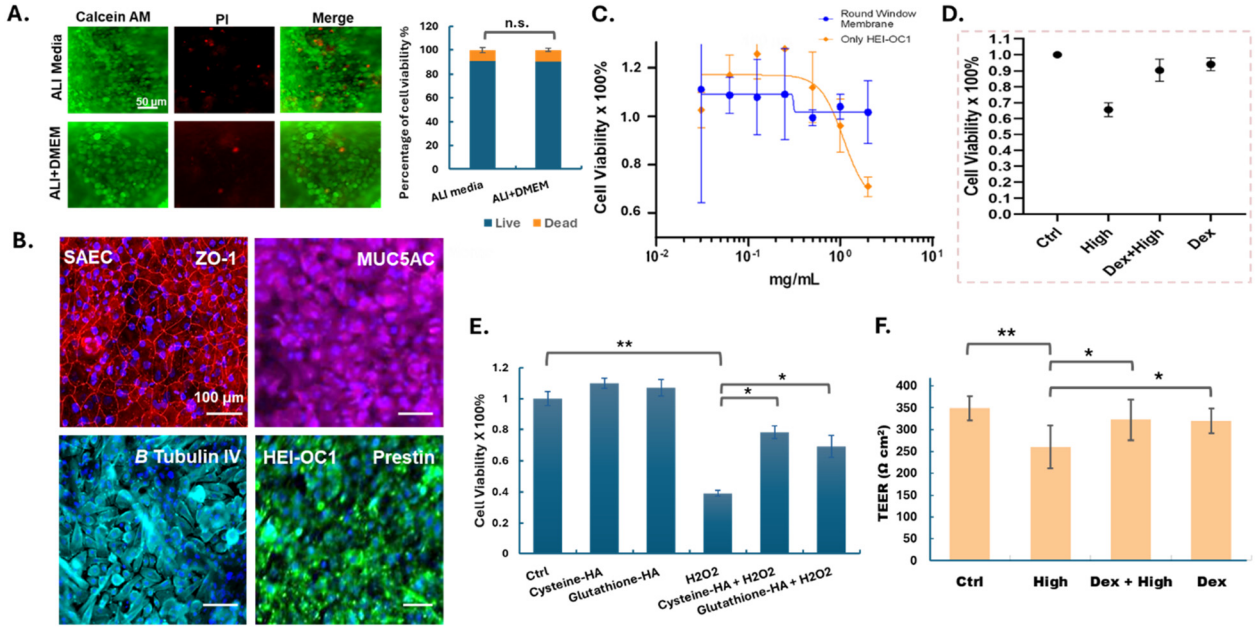

Fig. 5 Characterization of the coculture platform – RWM + sensory epithelial compartment (HEI-OC1 cells) and drug screening. A. Live/dead staining assay – hair cell viability in co-culture, in two different media (pneumatic-ALI-S alone or ALI-S + DMEM with 10% FBS). B. IF staining – hair cell/SAEC key marker expressions. C. Dexamethasone toxicity: dose response curve – anti-inflammatory drug toxicity to hair cells, with and without RWM cell types. D. Hair cell response: ototoxic injury model using acute inflammation and assessing hearing-loss preventive drugs responses. Proinflammatory cytokine cocktail treatment (High), dexamethasone alone (Dex) (0.5 mg mL^{-1}), or co-treatment of dexamethasone and the proinflammatory cytokine cocktails (Dex + High), RWM/cochlear cell coculture without treatment (Ctrl). E. Hair cell response: ototoxic injury model using excessive oxygen species and assessing hearing-loss preventive drugs responses. F. Analysis of barrier function using the integrated TEER sensor in the ototoxicity model and dexamethasone treatment. Proinflammatory cytokine cocktail treatment (High), dexamethasone alone (Dex) (0.5 mg mL^{-1}), or co-treatment of dexamethasone and the proinflammatory cytokine cocktails (Dex + High), RWM/cochlear cell coculture without treatment (Ctrl).

Although both MEEC and RPTEC are primary cells, there are crucial differences in their culture behavior and practical utility for model development. MEEC, derived from the middle ear, are highly sensitive to culture conditions, and the monolayer starts to deform after prolonged culture (Fig. S11C†). These factors make it difficult to achieve consistent and reproducible results, especially in long-term experiments or high-throughput applications. Due to the simpler cultural requirements, well-characterized for their robust growth and differentiation potential under defined culture conditions of RPTEC compared to MEEC, we have chosen to use RPTEC for RWM model development.

Testing anti-inflammatory and antioxidative drugs in the ototoxic MPS models

To characterize the RWM-hair cell coculture model, we used dexamethasone and first performed dose-dependent cell viability analysis. Eight to nine different drug concentrations were selected for testing. The CellTiter-Glo® Luminescent Cell Viability Assay was used to perform the dose-dependent cell viability analysis. We found that the concentration between 1–10 mg mL^{-1} was not sufficient to kill most of the cells at 48 hours (cell viability >50%) in the co-culture condition, however, HEI-OC1 cells alone are more vulnerable to the cytotoxicity effect caused by dexamethasone (Fig. 5C). We hypothesize that dexamethasone was metabolized by RWM cell types, and generated a less toxic derivative compound, as the only variable between the co-culture and the HEI-OC1 cell culture alone is the presence of RWM cells. The percentage of cell viability in the presence of drugs was compared to the control group (without drug treatment, 100%).

We then induced an ototoxic injury model by treating the MPS with a combination of proinflammatory cytokines: TNF-α, IL-6, IL-10, and IL-12p70 at 42, 16, 1.3, and 2.1 ng mL^{-1}, respectively, for 24 hours (High).[24] We either use dexamethasone alone (Dex) (0.5 mg mL^{-1}) or co-treatment of dexamethasone and the proinflammatory cytokine cocktails (Dex + High).[25] The experimental design can be found in Fig. S13.† The results suggested that the presence of the high-inflammation blend (High) significantly reduced cell viability (down to 65%) (Fig. 5D). And dexamethasone protected HEI-OC1 hair cells from inflammation-induced damage.

In addition, we also designed another ototoxic injury model with H_2O_2 to test the anti-oxidative compounds – glutathione–HA, and cysteine–HA. The experimental design can be found in Fig. S13.† H_2O_2 induced significant cell death for HEI-OC1 cells. After 24 hours of pretreatment, both glutathione–HA and cysteine–HA, tested at 1.5 mg mL^{-1} didn't exhibit any cytotoxicity for hair cells. Both glutathione–HA and cysteine–HA in the presence of H_2O_2 did exhibit significant protective effects

on oxidative damage (Fig. 5E) (from 37% to 65% and 76%, respectively). And our data aligned with the previous finding.[14] This indicates the establishment of a reliable co-culture model for testing hearing-protective drugs. The model allows for accurate evaluation of potential therapeutics in preventing or reducing damage to auditory cells. By utilizing this co-culture system, researchers can assess the efficacy and safety of hearing-protective drugs in a controlled and reproducible setting, providing valuable insights into their potential clinical applications.

RWM permeability analysis using integrated TEER and protein sensors in the MPS

TEER sensor measurement. The next step was to investigate the TEER measurement using the integrative TEER device in the presence of drugs. We used the same ototoxic injury model (proinflammatory condition) and drug treatment. The integrated TEER measurement showed a notable reduction in the measured value (Fig. 5F), indicating that the presence of the cytokine cocktail disrupts the integrity of the RWM, and in the presence of dexamethasone, a recovery of the measured value comparable to the control group was observed. This data is aligned with the cytotoxicity measurements (Fig. 5D). We also integrated a protein GFET sensor in our 32-unit device and assessed sensor efficacy by measuring TNF-α expression on-chip. The experiment layout and results can be found in Fig. S14.†

In this study, we have developed two versions of our system: one features TEER integration with 16 devices on a single plate, while the other incorporates a protein sensor, allowing for 32 devices in one plate. The TEER-integrated version enables to monitor epithelial barrier function development in continuous measurements, without sacrificing a sample and thus allowing "real-time" monitoring of the RWM construct progress. The protein sensor version, with a higher device capacity, is designed for detecting cytokine expressions such as cytokine levels, offering a more comprehensive view of cellular responses.

Looking ahead, our future work will focus on integrating both TEER and cytokine sensors into a single platform that fits the dimensions of a standard multi-well plate. This combined system will provide simultaneous monitoring of barrier function and inflammatory responses, making it an even more powerful tool for drug testing and mechanistic studies in microphysiological systems. The concept of MPS and sensor integration can also be applied to a wide range of drug discoveries for various disease types and allows us to gain a more comprehensive understanding of cellular response to various stimuli.

Experimental

Device fabrication

The device consists of an apical chamber, a PET membrane layer, a bottom layer, and biocompatible tape layers (AR 90106, medical grade pressure-sensitive adhesive, Adhesives Research, Ireland). The 3 mm polymethylmethacrylate (PMMA) (Astra Products, Copiague, NY) parts of the platform were designed in AutoCAD 2016 (Autodesk, Mill Valley, CA) for the apical chamber and the basal channel, converted to an Adobe Illustrator file (.ai), and finally fabricated by laser cutting using a VLS 3.50 desktop laser cutter (Universal Laser Systems, Scottsdale, AZ). PET membranes (0.4 μm pores, 12 μm thickness, SterliTech, Auburn, WA) and biocompatible tape layers were laser cut as well. The individual layers' layout was shown in Fig. 1B and the channel dimension was shown in Fig. S1,† and they were sandwich-assembled using biocompatible tapes with a device alignment holder. After assembly, the devices were held together using binder clips and placed in a 70 °C vacuum oven (VWR, Radnor, Pennsylvania) overnight. The following day, the devices underwent a 2-minute plasma treatment, followed by 20 minutes of UV sterilization. Before seeding cells, the device channels were hydrated with cell culture media (DMEM + 10% FBS).

Cell culture and maintenance

SAEC were cultured in airway epithelial cell basal media supplemented with bronchial epithelial cell growth kit components, HDF were grown in fibroblast basal media supplemented with fibroblast growth kit components (low serum), and RPTEC were grown in the renal epithelial cell basal media supplemented with renal epithelial cell growth kit components. All the reagents and cells were purchased from ATCC (Manassas, Virginia) unless otherwise stated. All the primary cells were used between passages 5 and 8. Cells were cultured at 37 °C with 5% CO_2 in a standard incubator. 0.05% of trypsin–EDTA was used for cell detachment, and the media was refreshed every other day. HEI-OC1 cells were from the University of California, Los Angeles (Dr. Federico Kalinec's lab), and were cultured at 33 °C with 10% CO_2 with DMEM + 10% fetal bovine serum (FBS). MEEC were purchased from ScienCell, Inc. (Carlsbad, CA), and were cultured in Epithelial Cell Medium-2 (ScienCell laboratory) at 37 °C with 5% CO_2. Cells beyond passage 7 (P7) were not used. THP-1 cells were cultured in floating condition using RPMI1604 (ATCC) + 10% FBS at 37 °C with 5% CO_2.

Device seeding

The PET membrane (the side facing the basal channel) in the device was first coated with 50 μg mL^{-1} collagen type I, dissolved in 0.01 M hydrochloric acid (HCl), and incubated at 37 °C for 1 hour. The basal channel was then washed once with sterile DI water and once with PBS. RPTEC cells (80 000 cells per device) were then seeded into the basal channel, and the device was flipped upside down and incubated in a humidity chamber at 37 °C and 5% CO_2 for 4 hours to allow cell attachment on the PET membrane. Afterward, the devices were flipped back, and the wells were filled with RPTEC culture medium.

On day 2, a 7.5% GelMA (CELLINK, Sweden) solution was prepared in 1× PBS, following the manufacturer's protocol. HDF were mixed with the GelMA solution to a final concentration of 1×10^5 cells per mL. 40 μL of the cell and gel mixture was applied to the apical chamber (the apical side of the membrane) in the device with RPTEC attached to the basal side of the membrane. UV crosslinking was performed for 10 seconds per device using a UV generator (MIDORI™ULB-50SC, Ushio, Cypress, CA). After gel cross-linking, the devices were returned to the hood and left for 10 minutes, followed by a 30-minute wash with fresh SAEC media. SAEC (80 000 cells per device) were then seeded on top of the GelMA + HDF layer. Additional SAEC media was added to the apical chamber, and RPTEC media was applied to the basal channel to support co-culture growth.

For air–liquid interface (ALI) culture, SAECs were grown until confluent. PneumaCult™-ALI-S Medium (STEMCELL Technologies, Cambridge, MA) was applied to both the apical chamber and basal channel for 24 hours, after which the media in the apical chamber was aspirated. Media changes were performed every 2–3 days in the basal channel. The RWM tissue was ready for use starting from day 14 post-ALI establishment.

For co-culture with auditory hair cells, on day 14 post-ALI establishment, HEI-OC1 cells (10 000 cells per device) were seeded into the basal channel. The device was incubated at 33 °C and 10% CO_2 for 48 hours to allow confluence before conducting drug testing.

Immunofluorescent staining and Live & Dead assay

The RWM cell types and the auditory hair cell type were stained with vimentin (ab92547), cytokeratin-5 (CK5, ab16570), cytokeratin-14 (CK14, ab7800), zonula occludens-1 (ZO-1, ab221547), MUC5AC (ab198294), and beta-tubulin IV (PA5-103158, Fisher Scientific, Waltham, MA) and prestin (ab242128). All the primary antibody was purchased from Abcam (Waltham, MA). Briefly, cell culture media in the device was removed, and cells were rinsed by 1× DPBS and fixed by 4% paraformaldehyde (PFA) (Fisher Scientific, Waltham, MA) for 15 min at room temperature. 0.1% Triton X-100 (Sigma-Aldrich, St. Louis, MO) was then applied for another 15 min prior to adding cell blocking solution (5% w/v BSA dissolved in 1× DPBS) for 1 h at room temperature. Then the cells were stained with primary antibodies overnight at 4 °C. On the next day, secondary antibodies (1 : 200) Alexa Fluor® 647 (goat anti-mouse IgG), Alexa Fluor® 488 (goat anti-chicken IgG) and Alexa Fluor® 594 goat anti-rabbit IgG), Invitrogen, Carlsbad, CA), were applied for 1 h at room temperature for the respective samples, followed by subsequent DPBS washing. Fluorescent images were obtained by fluorescent microscopy (Olympus (IX83), Tokyo, Japan) and Cytation 10 confocal imager (Agilent, Santa Clara, CA).

The cell viability was determined by calcein AM/propidium iodide Live & Dead staining (Invitrogen, Carlsbad, CA). For RWM cell types, we determined the cell viability of individual 3-cell layers. And quantification of alive and dead cell numbers has been conducted by ImageJ. The RGB images were first converted into binary black and white images (epithelial cells – monolayer; HDF – projection image of z-stack images, the z-stack was performed by taking approximately 25–30 slices at 5 μm thickness along the *z*-plane) for HDF. The image segmentation was used to count live and dead cells. For SAEC and RPTEC, instead of obtaining z-stack images, we used the fluorescent microscope to obtain single images of individual cell types.

TEER sensor device fabrication

Gold electrodes, which were used for TEER sensing, were fabricated directly on the apical and basal surfaces of the microfluidic flow region. A porous PET membrane was sandwiched between layers of pressure sensitive adhesive (PSA) and patterned PMMA sheets as substrates to assemble the TEER-incorporated multiplex chip are seeded directly on the PET membrane (0.4 μm pores, 12 μm thickness) or on the basal surface within the microfluidic flow region, so it was critical to consider sensor stability and biocompatibility under typical cell culture conditions. The sheets were rinsed with isopropanol, dried with a stream of compressed nitrogen gas, and exposed to oxygen plasma for 1 minute to remove any organic impurities. The apical and basal electrode patterns were designed in SolidWorks software and patterned onto a paper-based photomask. The patterned substrates underwent metallization and were coated sequentially with a 3 nm Cr (chromium) adhesion layer & a 25 nm Au (gold) conductive layer in a metal e-beam evaporator. The patterned gold was exposed to oxygen plasma to remove organic impurities. Gold-based electrodes were ultimately selected due to considerations for biocompatibility, inherent inertness, and high conductivity. To limit exposure to impurities, TEER sensors were fabricated in a class 100 cleanroom.

TEER measurements were obtained by performing Galvanostatic Electrochemical Impedance Spectroscopy (GEIS), in which the system is perturbed by a fixed current, and the voltage drop between two electrodes is measured.

The TEER value was calculated using the following formula:

$$\mathrm{TEER} = (R_1 - R_0) \times S$$

where R_1 is the measured value at a given time, R_0 is the measured value in the absence of cells, and S is the surface area of the cell culture. To analyze the impedance spectra of cellular systems, it is necessary to isolate the contributions to capacitance and resistance associated with the system. There are four key players: the ohmic resistance of tight junction proteins in the paracellular route (R_{TEER}), ohmic resistance of the cell membrane (R_{membrane}), the resistance of the cell culture medium (R_{medium}), capacitance of the cell membrane (C_{C}), and electrode capacitance (C_{E}). The value of R_{membrane} is so high, forcing current to pass *via* other paths, so its contribution is negligible within the equivalent circuit. The relationship

between cell resistance, cell culture medium resistance, the capacitance of the cell, and capacitance of the electrode are illustrated in an equivalent circuit by Srinivasan *et al.*[26]

Multiplex fluidic distributor design

The design of the fluidic distributor was attached to the top surface of the multiplexed plate and channel lengths reaching each device were designed to be equal to ensure the same hydraulic resistances for each device. After the CAD drawings (Autodesk, Mill Valley, CA), the layers were cut out of mylar sheets using a VLS 3.50 desktop laser cutter (Universal Laser Systems, Scottsdale, AZ). And the thickness of the individual layer was optimized.

Drug testing

For all the drug testing experiments unless stated, 200 μL of drug dissolved in 1× PBS was applied on each apical side of the already-formed RWM tissue model (14 days in ALI culture) and incubated for 48 h. Cell viability was assessed using calcein AM and propidium iodide following the manufacturer's protocol. The dose–response cell viability for four drugs—erythromycin, gentamycin, dexamethasone, and ciprofloxacin (the drugs are all from Millipore (Burlington, MA) unless otherwise stated) was calculated for each cell type, and a normalized value was determined by averaging across all three cell types.

TD_{50} is defined as the drug concentration that kills 50% of the cell population, normalized across all three cell types. A stock solution of the drug was prepared, and a concentration gradient with 8–9 different concentrations was generated. For the experiment, we used the CellTiter-Glo® Luminescent Cell Viability Assay from Promega (Madison, WI). Staurosporine (10 μM), a protein kinase C inhibitor, served as a positive control and effectively killed the majority of cells. We then tested ciprofloxacin at concentrations of 0.05 mg mL^{-1}, 0.1 mg mL^{-1}, 0.5 mg mL^{-1}, 1 mg mL^{-1}, 2.5 mg mL^{-1}, 5 mg mL^{-1}, 10 mg mL^{-1}, and 25 mg mL^{-1} to determine the TD_{50}. A serial dilution of the drug was performed using SAEC medium as the diluent to achieve the desired concentrations.

The lactate dehydrogenase (LDH) assay was performed according to the manufacturer's protocol. We used the fluorometric LDH reagent (ab197000, Abcam, Waltham, MA) that measures extracellular LDH in the cell culture medium through an enzymatic reaction that results in the formation of a red formazan product. After drug treatment, the cell culture media were harvested from both the apical chamber and basal channel in equal amounts, and the excitation/emission wavelengths of 535/587 nm were measured using a spectrophotometer to assess cellular membrane integrity.

Drug diffusion properties of dexamethasone and gentamicin were characterized using LC-MS at the University of Massachusetts Chan Medical School, Small Molecule Drug Screening Facility. 200 μL of 1 mg mL^{-1} drugs (dexamethasone and gentamicin) were added to the apical chamber and incubated for 48 hours. Sampling was taken at the basal channels at 24 h and 48 h (200 μL, each device only sampled once) and stored at −80 °C until analysis. Samples were analyzed on an Agilent Infinity 1260 LC-MS on a C18 (2.1 × 100 mm, 1.7 μm particle size) column.

The permeability coefficient (K_P) in m s^{-1} was calculated using the formula:[27]

$$K_p = \frac{Q}{A \cdot t \cdot (C_T - C_B)}$$

where Q is the mass in μg of substance transported through the RWM in time t in seconds across the RWM area A in m^2. The C_T and C_B are the concentrations in μg ml^{-1} on the top and bottom of the RWM.

Statistical analysis

For biochemical assays, each sample had four replicates unless otherwise noted. The statistical analyses of sample means were performed using GraphPad Prism software. One-way ANOVA, complemented by Tukey's pairwise comparisons, was used to evaluate group differences. A p-value less than 0.05 was considered statistically significant.

Conclusion

In conclusion, this study presents a significant advancement in the field of auditory research through the development of a novel multiplex 3D middle ear/cochlear-on-a-chip microphysiological system (MPS) model. By successfully integrating a three-layered round window membrane and auditory hair cell model within a microfluidic framework, we have created a reliable platform that not only mimics the physiological conditions of the middle-inner ear, but also the incorporation of multiplex devices, along with monitoring capabilities through TEER and GFET cytokine sensors, enhances the functionality and versatility of our model.

The initial toxicity screenings conducted with established therapeutics highlight the effectiveness of our RWM-on-a-chip model in assessing drug toxicity and calculating TD_{50} values, confirming its potential as a reliable testing platform.

Furthermore, the integration of HEI-OC1 hair cells allows for the exploration of drug responses to both common anti-inflammatory agents and innovative antioxidant compounds, paving the way for the identification of new therapeutic strategies. The successful assessment of drug diffusion across the RWM layer underscores the permeability of our model and its relevance to *in vivo* conditions.

Overall, this research not only addresses the current limitations of existing models but also provides a powerful tool for high-throughput screening of investigational new drugs. By minimizing reliance on animal models, our findings have important implications for the development of novel protective agents against hearing loss, contributing to advancements in auditory therapeutics and enhancing our understanding of inner ear drug response.

Data availability

The data generated in this study, including source data for the figures and details of methods and designs for the studies presented in the manuscript, are available upon publication and upon request from the corresponding author.

Author contributions

Jing Bai: investigation, methodology, conceptualization, formal analysis, visualization, writing. Olurotimi Bolonduro: investigation, methodology, formal analysis, writing. Pavlo Gordiichuk: investigation, methodology, formal analysis, writing. R. Madison Green: investigation, methodology, formal analysis, editing. Henry Hung-Li Chung: investigation, methodology, editing. Ken Mahmud: conceptualization, supervision, funding, resources, editing. Dmitry Shvartsman: resources, supervision, editing, conceptualization.

Conflicts of interest

There are no conflicts to declare.

Acknowledgements

Support for this project was provided by Contract No. N00014-21-C-2011 from the U.S. Department of Defense. We thank Dr. Monica A. Serban from the University of Montana for providing the two compounds: glutathione–HA and cysteine–HA.[14] We thank Dr. Federico Kalinec for providing HEI-OC1 cells.[13] Some images from Fig. 1 and 5 and Fig. S7† were created in **https://Biorender.com**.

References

1 W. H. O. WHO, Deafness and hearing loss, **https://www.who.int/news-room/fact-sheets/detail/deafness-and-hearing-loss**.
2 M. V. Goycoolea, *Acta Otolaryngol. Suppl.*, 1992, **493**, 43–55.
3 R. P. Cousins, PHARMACEUTICAL INTERVENTIONS FOR HEARING LOSS Newsletter, **https://hearing.health.mil/-/media/Files/HCE/Documents/PIHL-Newsletter_Winter-2018_Edition-7.pdf**.
4 S. S. Liu and R. Yang, *Front. Neurosci.*, 2022, **16**, 867453.
5 M. R. Bowl and S. J. Dawson, *Gerontology*, 2015, **61**, 149–157.
6 S. Han, H. Suzuki-Kerr, M. Suwantika, R. S. Telang, D. A. Gerneke, P. V. Anekal, P. Bird, S. M. Vlajkovic and P. R. Thorne, *J. Assoc. Res. Otolaryngol.*, 2021, **22**, 1–17.
7 F. G. Mondalek, Y. Y. Zhang, B. Kropp, R. D. Kopke, X. Ge, R. L. Jackson and K. J. Dormer, *J. Nanobiotechnol.*, 2006, **4**, 4.
8 Y. Hu, J. Xing, H. Zhang, X. Pang, Y. Zhai, H. Cheng, D. Xu, M. Liao, Y. Qi, D. Wu, B. Zhang, L. Cheng, B. Chu, C. Zhang, Y. Zhao and R. Chai, *Adv. Mater.*, 2024, **36**, 2309002.
9 M. Sekulic, N. Abdollahi, L. Graf, N. Deigendesch, R. Puche, D. Bodmer and V. Petkovic, *RSC Adv.*, 2023, **13**, 25508–25517.
10 L. Mou, K. Mandal, M. M. Mecwan, A. L. Hernandez, S. Maity, S. Sharma, R. D. Herculano, S. Kawakita, V. Jucaud, M. R. Dokmeci and A. Khademhosseini, *Lab Chip*, 2022, **22**, 3801–3816.
11 A. T. Young, K. R. Rivera, P. D. Erb and M. A. Daniele, *ACS Sens.*, 2019, **4**, 1454–1464.
12 A. Béraud, M. Sauvage, C. M. Bazán, M. Tie, A. Bencherif and D. Bouilly, *Analyst*, 2021, **146**, 403–428.
13 G. M. Kalinec, C. Park, P. Thein and F. Kalinec, *J. Visualized Exp.*, 2016(115), 54425.
14 E. Arrigali, J. Veit, B. Birru, J. Tine, K. Sandau, E. Barrett-Catton, Z. Tonnerre and M. Serban, *Front. Pharmacol.*, 2024, **15**, 1355279.
15 F. A. Abdel Baki, A. A. Omran, S. I. Asal and K. M. Hassan, *Egypt. J. Otolaryngol.*, 2017, **33**, 631–636.
16 A. Moatti, D. Silkstone, T. Martin, K. Abbey, K. A. Hutson, D. C. Fitzpatrick, C. J. Zdanski, A. G. Cheng, F. S. Ligler and A. Greenbaum, *iScience*, 2023, **26**, 106789.
17 Y. Wang and E. S. Olson, *Hear. Res.*, 2016, **337**, 1–11.
18 A. J. Hudspeth, *Neuron*, 2008, **59**, 530–545.
19 R. Singh, B. Birru, J. G. S. Veit, E. M. Arrigali and M. A. Serban, *Pharmaceuticals*, 2022, **15**, 1105.
20 M. V. Goycoolea, *Acta Oto-Laryngol.*, 2001, **121**, 437–447.
21 R. Singh, B. Birru, J. G. S. Veit, E. M. Arrigali and M. A. Serban, *Pharmaceuticals*, 2022, **15**, 1105.
22 FDA, FDA-Approved Labeling for CIPRO (Ciprofloxacin Hydrochloride) Tablets, **https://www.accessdata.fda.gov/drugsatfda_docs/label/2005/019537s057%2C020780s019lbl.pdf**.
23 T. Kloskowski, N. Gurtowska, J. Olkowska, J. M. Nowak, J. Adamowicz, J. Tworkiewicz, R. Dębski, A. Grzanka and T. Drewa, *Int. J. Oncol.*, 2012, **41**, 1943–1949.
24 B. Birru, J. Veit, E. Arrigali, J. Tine, E. Barrett-Catton, Z. Tonnerre, P. Diaz and M. Serban, *Front. Pharmacol.*, 2024, **15**, 1355283.
25 C. T. Dinh, E. Bas, S. S. Chan, J. N. Dinh, L. Vu and T. R. Van De Water, *Neuroscience*, 2011, **188**, 157–167.
26 B. Srinivasan, A. R. Kolli, M. B. Esch, H. E. Abaci, M. L. Shuler and J. J. Hickman, *J. Lab. Autom.*, 2015, **20**, 107–126.
27 C. M. Kelso, H. Watanabe, J. M. Wazen, T. Bucher, Z. J. Qian, E. S. Olson, J. W. Kysar and A. K. Lalwani, *Otol. Neurotol.*, 2015, **36**(4), 694–700.